medRxiv preprint doi: https://doi.org/10.1101/2025.05.23.25326669; this version posted May 23, 2025. The copyright holder for this preprint
(which was not certified by peer review) is the author/funder, who has granted medRxiv a license to display the preprint in perpetuity.
It is made available under a CC-BY-NC-ND 4.0 International license .

# *Title: Artificial Intelligence enhanced R1 maps can improve lesion detection in focal epilepsy in children*

*Authors list: Georgia Doumou[1], Felice D'Arco[2], Matteo Figini[3], Hongxiang Lin[3,4], Sara Lorio[1], Rory Piper[1,2] , Jonathan O'Muircheartaigh[5], J Helen Cross[2], Nikolaus Weiskopf[6,7,8], Daniel C Alexander[3], David W Carmichael[1]**

[1]Department of Imaging Physics & Engineering, School of Biomedical Engineering and Imaging Sciences, King's College London, London, UK.

[2]UCL Great Ormond Street Institute for Child Health, London, UK.

[3]Centre for Medical Image Computing, Department of Computer Science, University College London, London, UK.

[4]Research Center for Healthcare Data Science, Zhejiang Lab, Hangzhou, China.

[5]Department for Forensic and Neurodevelopmental Sciences, Institute of Psychiatry, Psychology and Neuroscience & Research Department of Early Life Imaging, School of Biomedical Engineering and Imaging Sciences, & MRC Centre for Neurodevelopmental Disorders, King's College London, London, UK

[6]Department of Neurophysics, Max Planck Institute for Human Cognitive and Brain Sciences, Leipzig, Germany.

[7]Felix Bloch Institute for Solid State Physics, Faculty of Physics and Earth Sciences, Leipzig University, Leipzig, Germany.

[8]Wellcome Centre for Human Neuroimaging, Institute of Neurology, University College London, 12 Queen Square, London WC1N 3AR, UK.

**Corresponding author*

***Abbreviations:***

*SNR = Signal-to-Noise Ratio*
*CNN = Convolutional Neural Networks*
*IQT = Image Quality Transfer*
*MCDs = Malformations of Cortical Development*
*FCD = Focal Cortical Dysplasia*
*MRI = Magnetic Resonance Imaging*
*GM = Gray Matter*
*WM = White Matter*
*MPM = Multi-Parameter Mapping (MPM)*
*HS = Hippocampal Sclerosis*

**NOTE: This preprint reports new research that has not been certified by peer review and should not be used to guide clinical practice.**

medRxiv preprint doi: https://doi.org/10.1101/2025.05.23.25326669; this version posted May 23, 2025. The copyright holder for this preprint
(which was not certified by peer review) is the author/funder, who has granted medRxiv a license to display the preprint in perpetuity.
It is made available under a CC-BY-NC-ND 4.0 International license .

**Acknowledgments:**

Thanks for the assistance of Dr Peter McColgan and Dr Kerrin Pine for their assistance in the training data collation.

**Funding:**

This work was supported by the Henry Smith Charity and Action Medical Research (GN2214) (D.W.C. and S.L.) and supported by the National Institute of Health Research (NIHR) Great Ormond Street Hospital Biomedical Research Centre. a BBSRC NPIF studentship (G.D.), and the Wellcome Trust core funding from the Wellcome EPSRC Centre for Medical Engineering at King's College London [WT203148/Z/16/Z]. J.O.M was funded by a Sir Henry Dale Fellowship jointly by the Wellcome Trust and the Royal Society (206675/Z/17/Z). R.J.P was funded by a Surgeon-Scientist grant by GOSCHCC (VS0221). N.W. received funding from the Deutsche Forschungsgemeinschaft (DFG, German Research Foundation) – project no. 347592254 (WE 5046/4-2) and the Federal Ministry of Education and Research (BMBF) under support code 01ED2210.

**Author contributions:**

Conceptualization: DWC, DCA
Methodology: GD, DCA, DWC, MF, HL, FD'A
Investigation: SL, GD, RP
Visualization: SFB, MJM, JLS, EH
Funding acquisition: DWC, HJC, DCA
Project administration: DWC, DCA
Supervision: SJ DWC, DCA, JOM
Writing – original draft: GCA, DWC
Writing – review & editing: GD, FD'A, MF, HL, SL, RP, JOM, JHC, NW, DCA, DWC

**Competing interests:**

The Max Planck Institute for Human Cognitive and Brain Sciences , KCL and UCL have an institutional research agreement with Siemens Healthcare. Siemens Healthcare provide research support to KCL including onsite scientists. Prof Nikolaus Weiskopf holds a patent on acquisition of MRI data during spoiler gradients (US 10,401,453 B2). NW was a speaker at an event organized by Siemens Healthcare and was reimbursed for the travel expenses.

**Data and materials availability:** All data, and materials are available on request to any researcher subject to any ethical or data protection restrictions. All code is freely available for any research, non-commercial purpose.

medRxiv preprint doi: https://doi.org/10.1101/2025.05.23.25326669; this version posted May 23, 2025. The copyright holder for this preprint
(which was not certified by peer review) is the author/funder, who has granted medRxiv a license to display the preprint in perpetuity.
It is made available under a CC-BY-NC-ND 4.0 International license .

# *Title: Artificial Intelligence enhanced R1 maps can improve lesion detection in focal epilepsy in children*

## *Abstract*

***Background and purpose:*** *MRI is critical for the detection of subtle cortical pathology in epilepsy surgery assessment. This can be aided by improved MRI quality and resolution using ultra-high field (7T). But poor access and long scan durations limit widespread use, particularly in a paediatric setting. AI-based learning approaches may provide similar information by enhancing data obtained with conventional MRI (3T). We used a convolutional neural network trained on matched 3T and 7T images to enhance quantitative R1-maps (longitudinal relaxation rate) obtained at 3T in paediatric epilepsy patients and to determine their potential clinical value for lesion identification.*

***Materials and Methods:*** *A 3D U-Net was trained using paired patches from 3T and 7T R1-maps from n=10 healthy volunteers. The trained network was applied to enhance paediatric focal epilepsy 3T R1 images from a different scanner/site (n=17 MRI lesion positive / n=14 MR-negative). Radiological review assessed image quality, as well as lesion identification and visualization of enhanced maps in comparison to the 3T R1-maps without clinical information. Lesion appearance was then compared to 3D-FLAIR.*

***Results:*** *AI enhanced R1 maps were superior in terms of image quality in comparison to the original 3T R1 maps, while preserving and enhancing the visibility of lesions. After exclusion of 5/31 patients (due to movement artefact or incomplete data), lesions were detected in AI Enhanced R1 maps for* ***14/15 (93%)*** *MR-positive and* ***4/11 (36%)*** *MR-negative patients.*

***Conclusion:***

medRxiv preprint doi: https://doi.org/10.1101/2025.05.23.25326669; this version posted May 23, 2025. The copyright holder for this preprint
**(which was not certified by peer review)** is the author/funder, who has granted medRxiv a license to display the preprint in perpetuity.
It is made available under a CC-BY-NC-ND 4.0 International license .

*AI enhanced R1 maps improved the visibility of lesions in MR positive patients, as well as providing higher sensitivity in the MR-negative group compared to either the original 3T R1-maps or 3D-FLAIR. This provides promising initial evidence that 3T quantitative maps can outperform conventional 3T imaging via enhancement by an AI model trained on 7T MRI data, without the need for pathology-specific information.*

medRxiv preprint doi: https://doi.org/10.1101/2025.05.23.25326669; this version posted May 23, 2025. The copyright holder for this preprint
(which was not certified by peer review) is the author/funder, who has granted medRxiv a license to display the preprint in perpetuity.
It is made available under a CC-BY-NC-ND 4.0 International license .

## *Introduction*

*The surgical treatment of focal epilepsy is the only current curative option available and should be considered early in the disease course if medication is ineffective[1]. Identification and accurate delineation of epileptic lesions such as Focal Cortical Dysplasia (FCD) using MRI plays a critical role in surgical evaluation particularly in a paediatric setting[2]. FCDs are often characterized by subtle GM cortical thickness extension and smoothed GM-WM borders not easily seen in conventional MRI[3]. Therefore, a considerable number of patients considered for epilepsy surgery do not have an MRI visible lesion[2] (termed 'MR negative') and this is associated with poor surgical outcome[4, 5]. 7T MRI has added value for epilepsy lesion identification and characterisation[6-8] via increased resolution and contrast[6] but has limited availability and is usually characterised by long acquisition times.*

*One intriguing possibility is the ability of artificial intelligence (AI) in visual learning tasks to enhance the appearance and resolution of MRI data. While AI models have been proposed to generate 7T-like MR images from 3T data, there are few demonstrations of 3T image enhancement in patients with brain abnormalities, and even less that address diagnostic yield. To achieve enhancement a neural network must be trained so that it contains the information necessary to accurately predict the high-resolution appearance of brain structure from low resolution data. Further, it is desirable for the resolution enhancement learnt to be generalisable – i.e. when presented with new data from a source different to that used for training it must retain accuracy of representation. These requirements often necessitate extremely large and varied datasets. Quantitative MRI maps are related to tissue properties regardless of acquisition sequence, hardware or other conditions[9]. This property makes maps highly reproducible across scanners (~1%[10] that could allow a network to be trained on quantitative MRI maps from one site and applied on new data from other sites with similar fidelity. Of those available, patch-based approaches are particularly interesting for clinical*

medRxiv preprint doi: https://doi.org/10.1101/2025.05.23.25326669; this version posted May 23, 2025. The copyright holder for this preprint
(which was not certified by peer review) is the author/funder, who has granted medRxiv a license to display the preprint in perpetuity.
It is made available under a CC-BY-NC-ND 4.0 International license .

*applications as they enable a single matched pair of images to provide many thousands of training examples dramatically reducing the need for large training datasets. Operating at this smaller scale may obviate the need for pathological training examples, where instead diversity across brain structures provides suitable generalisability relying on intensity transformations while operating below the scale of brain morphology.*

*Therefore, we artificially enhanced R1 (1/T1) maps using CNNs and Image Quality Transfer (IQT), methods that have previously shown promising results in image enhancement[11-17] and assessed their clinical value in focal epilepsy by investigating the following:* ***a)*** *Could the IQT pipeline trained only healthy control data be applied in epilepsy patients with cortical malformations previously detected by clinical MRI (MRI-lesion positive)?* ***b)*** *If so, do the AI enhanced R1 maps increase the visibility of the lesions in comparison to 3T R1 maps or conventional 3T FLAIR images?* ***c)*** *Can the AI enhanced R1 maps improve the sensitivity of lesion detection by aiding the identification of potential cortical abnormalities in clinical 3T MRI lesion negative cases?*

## *Materials and Methods*

*Our strategy consists of three main steps:* ***1)*** *Train a Convolutional Neural Network (CNN) variant based on a previously optimised network (classical 3D isotropic U-Net)[16,18,19] on healthy controls scanned both at 3T and 7T using established qMRI protocols[10, 20]. Healthy control subjects were used as they were able to tolerate the long 7T scan times. 2) Use the trained CNN network to enhance 3T data from a paediatric cohort with focal epilepsy including both MRI positive and negative cases,* ***3)*** *Assess the image quality and clinical radiological value.*

### *IQT Network Training*

medRxiv preprint doi: https://doi.org/10.1101/2025.05.23.25326669; this version posted May 23, 2025. The copyright holder for this preprint
(which was not certified by peer review) is the author/funder, who has granted medRxiv a license to display the preprint in perpetuity.
It is made available under a CC-BY-NC-ND 4.0 International license .

***Data acquisition***

*Quantitative R1 maps were obtained in n=10 healthy subjects (mean age 28 ± 4 years) at both 3T (1mm isotropic resolution) and 7T (0.5mm isotropic resolution) at the by Max Planck Institute for Human Cognitive and Brain Sciences, Leipzig, Germany (MPI-CBS) (DataMPI) using multi-parameter mapping (MPM) protocol based on 3D multi-echo GRE sequence acquisitions with variable flip angles[10,20,21].*

***Image processing***

*Images were processed with the hMRI toolbox[22] to generate 3T and 7T R1 maps. The 1mm resolution 3T R1 maps were coregistered and resliced (4th degree b-spline interpolation) to match the 0.5mm 7T resolution in SPM12. Brain masks were generated and applied to restrict the volume for training and reconstruction reducing computational requirements.*

***IQT network and training***

*The U-|Net was implemented in Python 3 using Keras library 2.3.1 (www.keras.io) with Tensorflow 1.5 (www.tensorflow.org) backend on a Nvidia Tesla V100 (32 GB). The 3T/7T R1 maps from each subject was used to create a library of paired 3T-to-7T patches using a sliding window to extract 32x32x32 patches with steps of 8x8x4 resulting in ~36500 patches in total. The patches with a percentage of >80% background voxels were excluded. Remaining patches were used to train the 3D U-Net[16,19]. The network was trained repeatedly where 9 subjects were used to train and a reconstruction was performed on the remaining unseen dataset to test its accuracy. The following parameters were used for all experiments following Lin et al[23]; ADAM (learning rate = 0.0001) was used as the optimizer and the pixel-wise mean squared error (MSE) as the loss function. For the convolutions (and up convolutions) 4 filters were used with 2x2x2 kernel size. An early stopping was set when the validation loss didn't decrease after*

medRxiv preprint doi: https://doi.org/10.1101/2025.05.23.25326669; this version posted May 23, 2025. The copyright holder for this preprint
(which was not certified by peer review) is the author/funder, who has granted medRxiv a license to display the preprint in perpetuity.
It is made available under a CC-BY-NC-ND 4.0 International license .

*10 epochs. Mean total training time was approximately 51 hours (epoch time ~ 3 hours), convergence was obtained after 14 epochs and validation MSE loss was 0.11.*

### *IQT Application in paediatric focal epilepsy*

#### *Data acquisition*

*The paediatric focal epilepsy group recruited consisted of n=33 (mean age 15±4 years) patients being evaluated for surgery at Great Ormond Street Hospital, UK (**Table 1 & Figure 1**). MPM data were incomplete for subjects 16 and 23 and therefore they were excluded from further analysis. The remaining n=31 subjects consisted of two cohorts; MR positives, where a lesion had been visually detected based on radiological review of images from a 3T epilepsy protocol (n=17) and MR negatives, where no lesion was visually detected (n=14) at the time of the MPM acquisition. One subject had a repeated scan (referred to as subjects 3 and 8). T Both scans were reconstructed and included for image quality analysis, but only one of them (subject 8) was used in the clinical evaluation. The following subjects were excluded from the lesion identification (see Figure 1); Subject 14 (severe motion artefacts); Subjects 1, 21 and 24 (incomplete electro-clinical data); Subject 15 (later diagnosed with genetic generalized epilepsy). Subject 27 was excluded from the comparison with 3D-FLAIR (3D-FLAIR was not retrievable).*

### *IQT Data analysis*

*Thirty-one R1 maps were enhanced applying the hyper-parameters and weights derived from the training on DataMPI to reconstruct AI Enhanced 3T R1 maps.*

### *Image quality assessment: 3T versus AI Enhanced R1 maps*

medRxiv preprint doi: https://doi.org/10.1101/2025.05.23.25326669; this version posted May 23, 2025. The copyright holder for this preprint
(which was not certified by peer review) is the author/funder, who has granted medRxiv a license to display the preprint in perpetuity.
It is made available under a CC-BY-NC-ND 4.0 International license .

*In a first review step, 3T and AI enhanced R1 maps were presented to a paediatric consultant neuro-radiologist with 10 years of experience (FD'A) in a randomized order blinded to any other clinical information including their status as MR-positive/negative. Images were assessed for GM-WM sharpness of the cerebrum, the cerebellum and the basal ganglia using a scale of 1-4 (1 (not visible), 2 (subtle), 3 (clear) or 4 (very clear)). The ranking results were statistically analysed using a non-parametric Wilcoxon test for 2 related samples in SPSS and frequency of the scores bar chart was generated. Significant differences were based on a threshold of $p<0.05$.*

***Epilepsy lesion identification: 3T versus AI Enhanced R1 maps***

*Next, both 3T and AI enhanced R1 maps were then reviewed for lesions blinded to any other electroclinical information. Lesion visibility was also scored using a scale of 1-4 (1 (not visible), 2 (subtle), 3 (clear) or 4 (very clear)).*

***Epilepsy lesion identification: Comparison to FLAIR***

*In a final review step 3T and AI enhanced R1 maps were presented together in a randomized patient order, unblinded to stratification information (MR positive/MR negative, MR localization if MR positive and EEG localization with a detailed description of the electro-clinical findings, including the suspected hemisphere and lobe). At this stage the maps were reviewed together with their clinical 3T 3D FLAIR[23](typically the best scan for lesion detection in epilepsy MRI protocols[24,25]) for comparison purposes. Lesions were scored for visibility using the scale described above for each image type.*

*Following this review process the number of lesions detected in the blinded and unblinded review were summarized in the MR positive and negative groups. Lesion visibility scores were also compared between the 3T and AI enhanced R1 maps and 3D FLAIR.*

medRxiv preprint doi: https://doi.org/10.1101/2025.05.23.25326669; this version posted May 23, 2025. The copyright holder for this preprint
(which was not certified by peer review) is the author/funder, who has granted medRxiv a license to display the preprint in perpetuity.
It is made available under a CC-BY-NC-ND 4.0 International license .

## *Results*

*Enhanced R1 maps were obtained in all of the 31 cases scanned. Enhanced images were of high quality and could be seen to contain pathological abnormalities present on the 3T maps that were not present in the healthy control adults training dataset (**Figure 2**).*

### *Image quality assessment: 3T versus AI Enhanced R1 maps*

*AI enhanced R1-maps had superior image quality compared to the original 3T R1-maps **(Figure 3, table 2)**. The Wilcoxon Signed Ranks test showed 31 positive ranks (AI Enhanced > 3T), no negative ranks (AI Enhanced < 3T) and no ties (AI Enhanced = 3T) for the cerebrum and the basal ganglia, and 27 positives, 4 negatives and no ties for the cerebellum.*

### *Epilepsy lesion identification in the MRI positive cohort*

### *3T versus AI Enhanced R1 maps*

*In the radiological review blinded to any additional clinical information, 3T R1 maps had lesions detected in 9 out of the 15 MRI positive cases, while 11/15 lesions were detected in the AI Enhanced R1 maps. The lesion visualization was scored better in 9/11 of the AI Enhanced maps compared to the 3T maps and equivalent in the remaining two cases. In the unblinded radiological review the identified lesion numbers increased to 13/15 and 14/15 for the 3T and AI Enhanced R1 maps, respectively.*

### *Comparison to 3D-FLAIR*

*Lesion visualization was assessed in 14 MR positive subjects comparing the 3T R1 maps, AI enhanced maps to clinical 3D-FLAIR unblinded (with additional electroclinical information provided). The visualization of lesions was better in the AI Enhanced R1map compared to the 3D-FLAIR in 6/14 **(see examples in fig. 4A and 4B)** (1 out of these 6 was judged as 'not visible'*

medRxiv preprint doi: https://doi.org/10.1101/2025.05.23.25326669; this version posted May 23, 2025. The copyright holder for this preprint
(which was not certified by peer review) is the author/funder, who has granted medRxiv a license to display the preprint in perpetuity.
It is made available under a CC-BY-NC-ND 4.0 International license .

*on the 3D-FLAIR **fig. 4C**); 5/14 were the same and in the remaining 3/14 visualisation was judged as worse than the 3D-FLAIR (in 1 out of these 3 was judged as 'not visible' on AI Enhanced). The visualization of lesions was worse on the 3T R1 maps compared to 3D-FLAIR. In 2/14 it was better (1 of 2 was judged as 'not visible' on FLAIR), 7/14 the same and in 5/14 it was worse (of which two were 'not visible').*

***Epilepsy lesion identification in the MRI negative cohort***

*In the blinded radiological review in the MRI negative cohort, lesions were not detected in the 3T R1 maps, however, in 4/11 cases lesions were identified in the AI Enhanced R1 maps (**subjects 7, 13, 26, 29**).*

***Comparison to 3D-FLAIR***

*Unblinded review of R1 maps and comparison of AI enhanced R1 maps to 3D-FLAIR (**table 3** green): Seven out of 11 had no lesion identified on the 3D-FLAIR nor the R1 maps (1 of these 7 (**subject 18**) was noted as suspicious for transmantle sign in left mesial frontal on the AI Enhanced map). For the 4 cases with lesions identified, in 3 the AI enhanced map was superior to the FLAIR which was scored as 'not visible' as was the 3T R1 map. However, the AI Enhanced maps were scored as having 'subtle' lesions (**fig. 5A (subject 7), 5B (subject 13) and 5C (subject 26)**). In the remaining MR negative case (**fig. 5D (subject 29)**) where a lesion was detected both the 3D-FLAIR and AI enhanced maps were scored as having a 'subtle' lesion while the 3T R1 map was 'negative'.*

*In these 4 MR negative cases, Subject 7 had a left frontal lesion detected which was concordant with SEEG and resection. Follow up 3T clinical MRI remained negative. Subject 13 had a left frontal lesion detected which was concordant with scalp EEG and a follow up repeat clinical 3T MRI. In subjects 26 and 29, lesions were concordant with EEG and seizure semiology, but no further investigations were performed to confirm these results.*

medRxiv preprint doi: https://doi.org/10.1101/2025.05.23.25326669; this version posted May 23, 2025. The copyright holder for this preprint
(which was not certified by peer review) is the author/funder, who has granted medRxiv a license to display the preprint in perpetuity.
It is made available under a CC-BY-NC-ND 4.0 International license .

## *Discussion*

*We aimed to improve image quality by creating high resolution AI enhanced R1 maps from lower resolution 3T R1 maps using a U-Net patch-based IQT network trained on data from a group of ten healthy individuals scanned at both 3T (1mm) and 7T (0.5mm). AI enhanced R1 maps were then generated in a cohort of paediatric epilepsy patients (separate scanner and site), exploiting the cross-site consistency of quantitative maps[10,26]. The clinical impact of the AI enhancement was evaluated on this paediatric epilepsy cohort consisting of both MR positive and MR negative patients with electro-clinical features consistent with MCD.*

*We firstly determined if the AI enhanced R1 maps had improved image quality, and that the trained network could generalize to the test dataset. Radiological assessment of image quality in the cerebrum, basal ganglia and cerebellum showed that the AI enhanced images scored significantly higher than the 3T R1 maps (**fig. 3**). We then evaluated, if imaging abnormalities were faithfully reconstructed in the AI enhanced images. In the 14 of 15 paediatric patients with visible lesions (MR-positive cohort) the enhanced images were able to preserve the pathological features even though there were no pathological cases in the training dataset of healthy adults (see examples in **fig. 4**). In the remaining subject the lesion identified in the clinical report was not confirmed by our expert rater (FD'A) on 3D-FLAIR.*

*Secondly, we determined if lesion visibility was enhanced in MR positive cases and if the enhanced R1 maps might increase the yield of lesion detection in MR negative cases. The lesion identification and visualization assessment within the MR positive cohort showed that the AI Enhanced R1 maps were always either superior (11/15) or equivalent to (4/15) the 3T R1 maps. The AI enhanced R1 maps enabled the expert reviewer to identify 4 new lesions out of the 11 MR-negative patients (the newly detected abnormalities were not visible in the original 3T R1 maps in all cases and were not visible in the 3D-FLAIR in 3/4). In one further case the AI*

medRxiv preprint doi: https://doi.org/10.1101/2025.05.23.25326669; this version posted May 23, 2025. The copyright holder for this preprint
(which was not certified by peer review) is the author/funder, who has granted medRxiv a license to display the preprint in perpetuity.
It is made available under a CC-BY-NC-ND 4.0 International license .

*enhanced map showed some indication of a transmantle sign, an abnormality associated with FCD IIb but it was not judged clear enough to be classified as a lesion.*

*Finally, we compared the lesion visibility in the maps to the clinical 'gold standard' 3T 3D-FLAIR image. The AI enhanced images had improved visibility in 6/14, similar in 5/14 and worse in 3/14. In the MR negative cohort 4 of 11 lesions were identified on the AI Enhanced R1 maps; only 1 of these 4 was also judged to be 'subtle' on the 3D-FLAIR. Validation of these new results in the four MR negative patients is challenging because relatively few of these patients go on to have surgery. The localisation of 1 of 4 lesions identified on the 3T Enhanced was concordant with SEEG findings and resection area with ILAE I seizure outcome following surgical resection (**subject 7**). In a further subject the localisation was concordant with EEG and a subsequent repeat clinical MRI (**subject 13**). In the remaining two MR negative patients with new findings the abnormalities were concordant with EEG but they did not have further investigation with SEEG or resective surgery (**subject 26** and **29**).*

*Some previous studies have utilised 3T T1 or R1 maps to detect abnormalities in FCD[3,27,28] although limited proven benefit for lesion detection in MRI negative cases was found[29]. Increased T1 values are correlated with baseline myelination and susceptible to microstructural damage likely to disrupted myeloarchitecture[30]. Here, we utilised R1 maps primarily to allow for IQT network training on 3T and 7T data from one site to be used on paediatric data from another, leveraging the high cross-site reproducibility of quantitative methods[10] that remove hardware specific influences. IQT, being patched based, was then able to generalise to the new data despite a small training dataset from 10 healthy individuals scanned at both field strengths.*

*Multiple features contributed to the improved radiological visualisation; in addition to increased resolution, the AI enhanced maps had reduced noise and motion artefacts that were*

medRxiv preprint doi: https://doi.org/10.1101/2025.05.23.25326669; this version posted May 23, 2025. The copyright holder for this preprint
(which was not certified by peer review) is the author/funder, who has granted medRxiv a license to display the preprint in perpetuity.
It is made available under a CC-BY-NC-ND 4.0 International license .

*not in the training data (**Fig 6**). Training data limitations were transferred to the enhanced maps including bright vessels owing to the 7T head transmit coil and low B1 transmit fields in the cerebellum that could be mitigated using parallel transmit approaches[31].*

*Using AI to enhance 3T R1 maps showed a yield of 14/15 (93%) lesions in the MR positive cohort, in the remaining case the clinically reported lesion was not confirmed by our expert in any scans. In 4/11 (36%), MR negative patients, lesions were detected, a similar yield to direct 7T imaging studies with ranges from 17-44%[4,32-34]. Interestingly, 3 out of 4 were consistent with electro-clinical information but judged not visible on clinical 3T 3D-FLAIR images even when guided by the AI enhanced R1 map; none were detectable on the 3T R1 maps highlighting that a genuine and clinically relevant image quality improvement had been achieved. The ability to enhance 3T data has advantages over UHF imaging owing to reduced cost and increased availability. Limited validation of new findings was possible owing to the rarity of surgery and SEEG in MR negative subjects that requires a larger prospective study. It would be possible to enhance 3D-FLAIR images, however signal features related to imaging parameters and hardware reduce generalisability across sites. While focal epilepsy was the application here, the approach is readily applicable to a wide range of potential patient groups where enhanced image quality could impact patient management.*

## *References*

1. *Skirrow C, et al Determinants of IQ outcome after focal epilepsy surgery in childhood: A longitudinal case-control neuroimaging study. Epilepsia. 2019 May;60(5):872-884*
2. *Krucoff MO, et al. Rates and predictors of success and failure in repeat epilepsy surgery: A meta-analysis and systematic review. Epilepsia. 2017 Dec;58(12):2133-2142*
3. *Nöth U, et al. Detection of cortical malformations using enhanced synthetic contrast images derived from quantitative T1 maps. NMR Biomed. 2020 Feb;33(2):e4203*
4. *Sharma HK, et al. Utility of 7 tesla MRI brain in 16 "MRI Negative" epilepsy patients and their surgical outcomes. Epilepsy Behav Rep. 2021 Jan 7;15:100424.*

medRxiv preprint doi: https://doi.org/10.1101/2025.05.23.25326669; this version posted May 23, 2025. The copyright holder for this preprint
(which was not certified by peer review) is the author/funder, who has granted medRxiv a license to display the preprint in perpetuity.
It is made available under a CC-BY-NC-ND 4.0 International license .

5. *Téllez-Zenteno JF, et al. Surgical outcomes in lesional and non-lesional epilepsy: a systematic review and meta-analysis. Epilepsy Res. 2010 May;89(2-3):310-8*
6. *Guye, M, et al. Malformations of cortical development: The role of 7-Tesla magnetic resonance imaging in diagnosis. Rev Neurol (Paris). 2019 Mar;175(3):157-162*
7. *Rados M, et al. Diagnostic value of MRI in the presurgical evaluation of patients with epilepsy: influence of field strength and sequence selection: a systematic review and meta-analysis from the E-PILEPSY Consortium. Epileptic Disord. 2022 Apr 1;24(2):323-342*
8. *Wang ZI, et al. Radiological and Clinical Value of 7T MRI for Evaluating 3T-Visible Lesions in Pharmacoresistant Focal Epilepsies. Front Neurol. 2021 Mar 2;12:591586*
9. *Adler S, et al. Towards in vivo focal cortical dysplasia phenotyping using quantitative MRI. Neuroimage Clin. 2017 Apr 20;15:95-105*
10. *Weiskopf N, et al. Quantitative multi-parameter mapping of R1, PD(*), MT, and R2(*) at 3T: a multi-center validation. Front Neurosci. 2013 Jun 10;7:95*
11. *Alexander DC, et al. Image quality transfer via random forest regression: applications in diffusion MRI. Med Image Comput Comput Assist Interv. 2014;17(Pt 3):225-32*
12. *Alexander DC, et al. Image quality transfer and applications in diffusion MRI. Neuroimage. 2017 May 15;152:283-298*
13. *Tanno R, Ghosh A, Grussu F, Kaden E, et al. Bayesian Image Quality Transfer. 2016. In: MICCAI 2016. LNCS 9901, 265–273. Springer, Cham*
14. *Tanno R, Worrall DE, Kaden E, Ghosh A, et al. Uncertainty modelling in deep learning for safer neuroimage enhancement: Demonstration in diffusion MRI. Neuroimage. 2021 Jan 15;225:117366*
15. *Lin H, et al. Deep learning for low-field to high-field MR: image quality transfer with probabilistic decimation simulator. 2019. In: Knoll F, Maier A, Rueckert D, Ye JC. (eds.) MLMIR 2019. LNCS, vol. 11905, 58–70. Springer, Cham*
16. *Lin H, et al. Low-field magnetic resonance image enhancement via stochastic image quality transfer. Med Image Anal. 2023 Jul;87:102807*
17. *Figini M, et al. Evaluation of epilepsy lesion visualisation enhancement in low-field MRI using image quality transfer: a preliminary investigation of clinical potential for applications in developing countries. Neuroradiology. 2024 Dec;66(12):2243-2252*
18. *Ronneberger, et al. (2015). U-Net: Convolutional Networks for Biomedical Image Segmentation. LNCS. 9351. 234-241. 10.1007/978-3-319-24574-4_28*

medRxiv preprint doi: https://doi.org/10.1101/2025.05.23.25326669; this version posted May 23, 2025. The copyright holder for this preprint
(which was not certified by peer review) is the author/funder, who has granted medRxiv a license to display the preprint in perpetuity.
It is made available under a CC-BY-NC-ND 4.0 International license .

19. *Çiçek Ö, Abdulkadir A, Lienkamp S.S, Brox T, Ronneberger O. 3D U-Net: learning dense volumetric segmentation from sparse annotation. 2016. In: Ourselin, S., Joskowicz, L., Sabuncu, M.R., Unal, G., Wells, W. (eds.) MICCAI 2016. LNCS, 9901, 424–432. Springer, Cham*
20. *Vaculčiaková L, et al. Combining navigator and optical prospective motion correction for high-quality 500 µm resolution quantitative multi-parameter mapping at 7T. Magn Reson Med. 2022 Aug;88(2):787-801*
21. *Weiskopf N, et al. Quantitative magnetic resonance imaging of brain anatomy and in vivo histology. 2021. Nat Rev Phys 3, 570–588*
22. *Tabelow K, et al. hMRI - A toolbox for quantitative MRI in neuroscience and clinical research. Neuroimage. 2019 Jul 1;194:191-210*
23. *Lorio S, Adler S, Gunny R, D'Arco F, et al. MRI profiling of focal cortical dysplasia using multi-compartment diffusion models. Epilepsia. 2020 Mar;61(3):433-444*
24. *Wang I, et al. MRI essentials in epileptology: a review from the ILAE Imaging Taskforce. Epileptic Disord. 2020 Aug 1;22(4):421-437*
25. *Bernasconi A, et al. Recommendations for the use of structural magnetic resonance imaging in the care of patients with epilepsy: A consensus report from the International League Against Epilepsy Neuroimaging Task Force. Epilepsia. 2019 Jun;60(6):1054-1068*
26. *Leutritz T, et al. Multiparameter mapping of relaxation (R1, R2*), proton density and magnetization transfer saturation at 3 T: A multicenter dual-vendor reproducibility and repeatability study. Hum Brain Mapp. 2020 Oct 15;41(15):4232-4247*
27. *Seiler A, et al. Multiparametric Quantitative MRI in Neurological Diseases. Front Neurol. 2021 Mar 8;12:640239*
28. *Su TY, et al. Evaluating whole-brain tissue-property changes in MRI-negative pharmacoresistant focal epilepsies using MR fingerprinting. Epilepsia. 2023 Feb;64(2):430-442*
29. *Hamid C, et al. Focal epilepsy without overt epileptogenic lesions: no evidence of microstructural brain tissue damage in multi-parametric quantitative MRI. Front Neurol. 2023 Jul 17;14:1175971*
30. *Hogan RE. Quantitative Measurement of Longitudinal Relaxation Time (qT1) Mapping in TLE: A Marker for Intracortical Microstructure? Epilepsy Curr. 2017 Nov-Dec;17(6):358-360*

medRxiv preprint doi: https://doi.org/10.1101/2025.05.23.25326669; this version posted May 23, 2025. The copyright holder for this preprint
**(which was not certified by peer review)** is the author/funder, who has granted medRxiv a license to display the preprint in perpetuity.
It is made available under a CC-BY-NC-ND 4.0 International license .

31. *Padormo F, et al. Parallel transmission for ultrahigh-field imaging. NMR Biomed. 2016 Sep;29(9):1145-61*
32. *Casella C, et al Widespread, depth-dependent microstructural alterations in the cortex of children with drug-resistant focal epilepsy: a quantitative T1 and T2 mapping study Archives of Disease in Childhood. 2023;108:A196-A197*
33. *Wang I, et al. Value of 7T MRI and post-processing in patients with nonlesional 3T MRI undergoing epilepsy presurgical evaluation. Epilepsia. 2020 Nov;61(11):2509-2520*
34. *Chen C, et al. 7T MRI with post-processing for the presurgical evaluation of pharmacoresistant focal epilepsy. Ther Adv Neurol Disord. 2021 Jun 8;14:17562864211021181*

medRxiv preprint doi: https://doi.org/10.1101/2025.05.23.25326669; this version posted May 23, 2025. The copyright holder for this preprint
**(which was not certified by peer review)** is the author/funder, who has granted medRxiv a license to display the preprint in perpetuity.
It is made available under a CC-BY-NC-ND 4.0 International license .

**Acknowledgments:**

Thanks for the assistance of Dr P McC and Dr K P for their assistance in the training data collation.

medRxiv preprint doi: https://doi.org/10.1101/2025.05.23.25326669; this version posted May 23, 2025. The copyright holder for this preprint
(which was not certified by peer review) is the author/funder, who has granted medRxiv a license to display the preprint in perpetuity.
It is made available under a CC-BY-NC-ND 4.0 International license .

## Figures

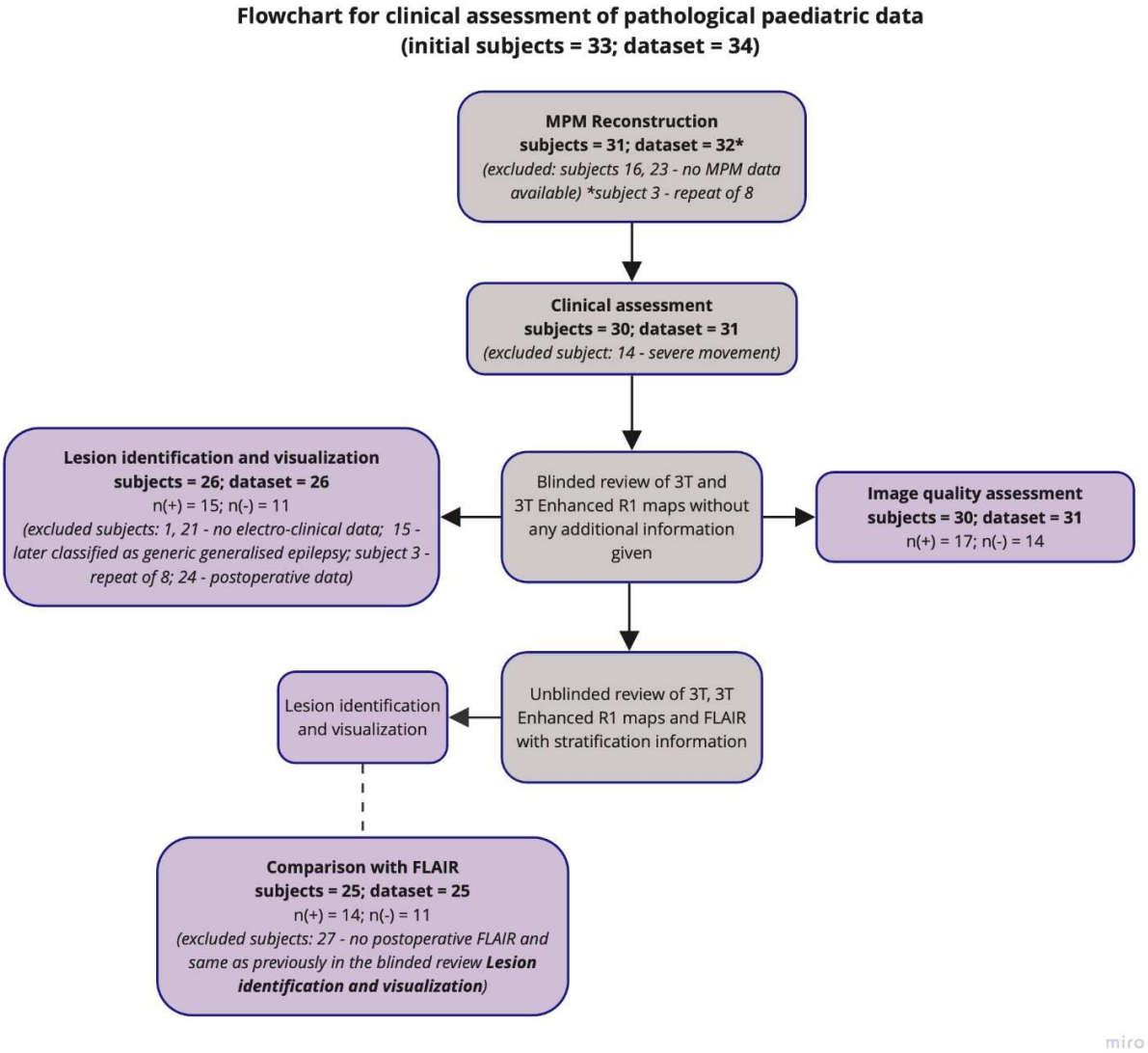



***Fig. 1*** *The flowchart includes the initial number of participants, those excluded for any reason, as well as the final numbers used for each analysis.*

medRxiv preprint doi: https://doi.org/10.1101/2025.05.23.25326669; this version posted May 23, 2025. The copyright holder for this preprint (which was not certified by peer review) is the author/funder, who has granted medRxiv a license to display the preprint in perpetuity. It is made available under a CC-BY-NC-ND 4.0 International license .

| Subject | Gender | Age | Age of onset | MRI neg=0 pos=1 | MRI Localisation | EEG Localisation | EEG Site | SEEG | Surgery | Resection area | Histology |
|---|---|---|---|---|---|---|---|---|---|---|---|
| 1 | M | 16–20 | NA | 0 | NA | N | NA | N | N | NA | NA |
| 2 | F | 16–20 | 6–10 | 1 | Bilateral periventricular heterotopia | Y | Left occipital, Left centro-parietal | N | Y | Laser ablation nodula heterotopia | No diagnostic findings |
| 3* (repeated subject 8) | M | 16–20 | 6–10 | 1 | Left frontal gyrus / Motor | N | Generalised EEG discharges | N | N | NA | NA |
| 4 | M | 16–20 | 11–15 | 0 | NA | Y | Multiple sites: Left frontal + Left posterior | N | N | NA | NA |
| 5 | F | 16–20 | 1–5 | 0 | NA | Y | Left temporal | N | Y | Left temporal lobe resection, Hippocampus, temporal neocortex | No diagnostic findings |
| 6 | F | 16–20 | 1–5 | 0 | NA | Y | Left frontal | Y | Y | Left frontal lobectomy, Left middle frontal gyrial lesion | No diagnostic findings |
| 7 | F | 16–20 | 6–10 | 0 | NA | Y | Right frontal | Y | Y | Right frontal cortical malformation. Left frontal resection after SEEG | Reactive gliosis |
| 8 | M | 16–20 | 6–10 | 1 | Left frontal gyrus / Motor | N | Generalised EEG discharges | N | N | NA | NA |
| 9 | F | 16–20 | 1–5 | 1 | Left parietal mesial, posterior of cingulate | N | NA | N | Y | Left temporal neo-cortex, hippocampus | HS |
| 10 | M | 11–15 | 1–5 | 1 | Left parietal mesial, posterior of cingulate | N | NA | N | Y | Left HS | HS |
| 11 | F | 11–15 | 1–5 | 0 | NA | N | Right centrotemporal+right frontal | N | N | NA | NA |
| 12 | F | 6–10 | 1–5 | 1 | Left insula | Y | Left sided predominance | N | Y | Left insula | FCD IIb |
| 13 | M | 11–15 | 6–10 | 0 | NA | N | Left onset with midline/Left upper frontal | N | N | NA | NA |
| 14 | F | 11–15 | 1–5 | 0 | NA | N | Left posterior (wide area) | Y | Y | Left middle and posterior temporal | FCD IIb |
| 15 | M | 11–15 | 11–15 | 0 | NA | Y | Both hemispheres | N | N | NA | NOT FOCAL later confirmed genetic abormality - improved with AED removal |
| 17 | F | 16–20 | 6–10 | 1 | Atrophy of right frontal lobe and operculum | Y | Right anterior (wide area) | N | N | NA | NA |
| 18 | M | 16–20 | 11–15 | 0 | NA | Y | Multiple sites: Left frontal + Left posterior | Y | N | NA | NA |
| 19 | F | 6–10 | 6–10 | 0 | NA | Y | Right central + Right frontal + Right temporal (subtle multifocal spike discharges) | N | N | NA | NA |
| 20 | M | 11–15 | 11–15 | 0 | NA | Y | Left parietal | Y | N | NA | NA |
| 21 | F | 11–15 | NA | 0 | NA | N | NA | N | N | NA | NA |
| 22 | M | 11–15 | 6–10 | 1 | Right post temporal and parietal region | Y | Right post temporal and centro-parietal region | N | Y | Right parietal | Low grade glioma/glioneuronal tumour |
| 24 | M | 11–15 | 6–10 | 1 | Polymicrogyria | Y | Right hemisphere | N | Y | Right frontal | FCD, PMG, leptominingeal heterotopia and white WM heterotopia |
| 25 | M | 11–15 | 1–5 | 1 | Right post insula | Y | Right post insula | N | N | NA | NA |
| 26 | M | 16–20 | 6–10 | 0 | NA | Y | Left frontal, left anterior quadrant | N | N | NA | NA |
| 27 | F | 6–10 | 1–5 | 1 | Right frontal lobe | Y | Right frontal | N | Y | Right frontal tuber | TS, TSC1 mutation |
| 28 | M | 16–20 | 1–5 | 1 | Left paracentral | Y | Left paracentral | N | Y | Left resection - incomplete | FCD IIb |
| 29 | M | 11–15 | 6–10 | 0 | NA | N | Right hemisphere (frontal temporal) | N | N | NA | NA |
| 30 | M | 11–15 | 1–5 | 1 | Left superior frontal sulcus at the juction with left precentral sulcus | Y | Left central | N | Y | Left motor cortex, Left frontal | No diagnostic findings |
| 31 | F | 16–20 | 11–15 | 1 | Left middle temporal gyrus | Y | Left middle temporal gyrus | N | Y | Left middle temporal lesion | Pleomorphic xanthoastrocytoma (PXA), WHO grade II, BRAF V600E mutation |
| 32 | F | 16–20 | 6–10 | 1 | Atrophy of right frontoparietal and insular lobes | Y | Right central/parietal + Right posterior/parietal temporal | N | Y | Right frontal cortex | Encephalitis (or polioencephalitis), other findings not specific for epilepsy |
| 33 | F | 11–15 | 1–5 | 1 | Mature gliotic damage in left middle cerebral artery | Y | Left insula | N | N | NA | NA |
| 34 | M | 11–15 | 6–10 | 1 | HS and left inferior frontal gyrus | Y | Left insula | N | Y | NA | HS |

***Table 1**: Demographic and clinical data of the pathological paediatric population*

medRxiv preprint doi: https://doi.org/10.1101/2025.05.23.25326669; this version posted May 23, 2025. The copyright holder for this preprint
(which was not certified by peer review) is the author/funder, who has granted medRxiv a license to display the preprint in perpetuity.
It is made available under a CC-BY-NC-ND 4.0 International license .

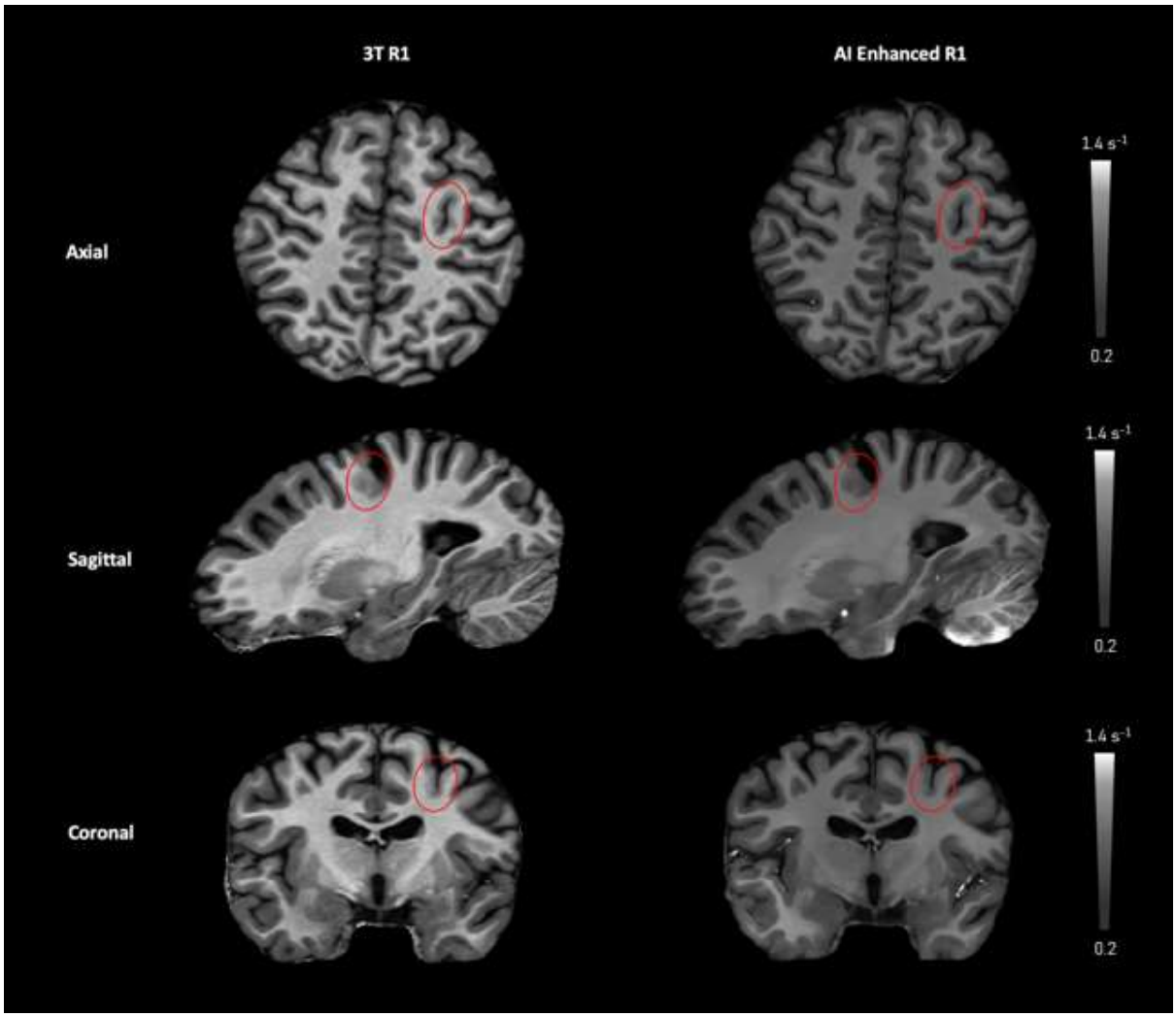



**Fig. 2:** Lesion identified in subject 8 in axial, sagittal and coronal view for the 3T (left) and AI Enhanced (right) R1 maps. Note images are scaled to quantitative units ($s^{-1}$) and R1 values are smaller at 7T than 3T so maps appear darker.

medRxiv preprint doi: https://doi.org/10.1101/2025.05.23.25326669; this version posted May 23, 2025. The copyright holder for this preprint
(which was not certified by peer review) is the author/funder, who has granted medRxiv a license to display the preprint in perpetuity.
It is made available under a CC-BY-NC-ND 4.0 International license .

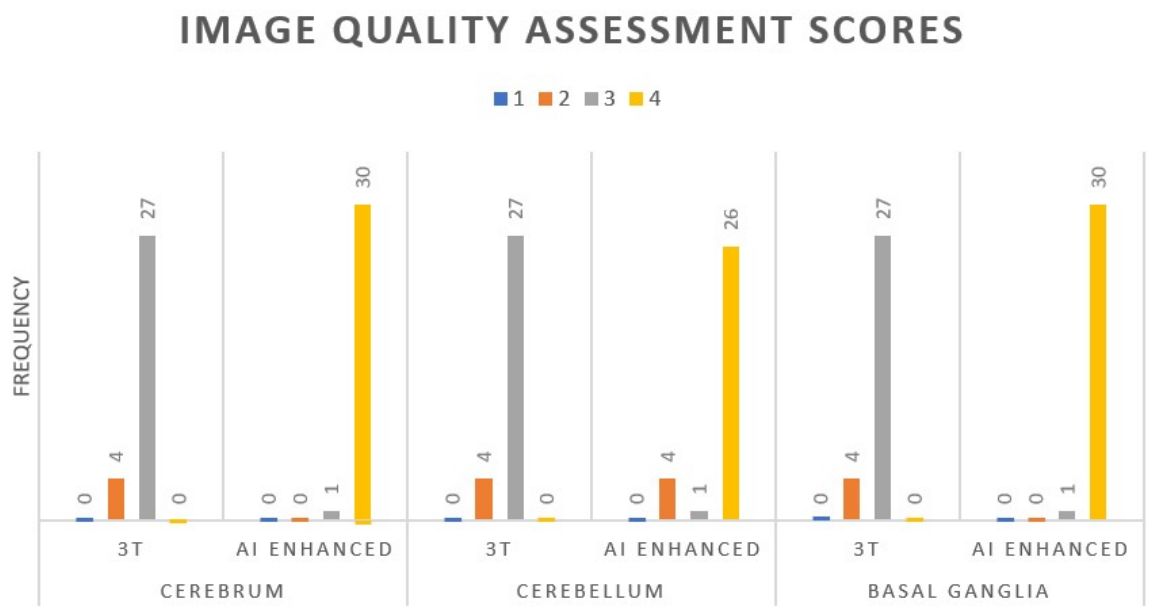



**Fig. 3:** Bar chart for the radiological image quality assessment scores frequency (y axis) for the 3T and the 3T Enhanced R1 maps in the cerebrum, cerebellum and basal ganglia. 1-4 (1 (not visible), 2 (subtle), 3 (clear) or 4 (very clear)).

| Image Quality Assesment Score | Interprestation |
|---|---|
| 1 | not visible |
| 2 | subtle |
| 3 | clear |
| 4 | very clear |

***Table 2**: Image Quality Assessment Scores and Their Interpretations*

medRxiv preprint doi: https://doi.org/10.1101/2025.05.23.25326669; this version posted May 23, 2025. The copyright holder for this preprint
**(which was not certified by peer review)** is the author/funder, who has granted medRxiv a license to display the preprint in perpetuity.
It is made available under a CC-BY-NC-ND 4.0 International license .

| Subject | FLAIR | 3T R1 | 3T Enahnced R1 |
|---|---|---|---|
| 2 | **clear** | subtle | **clear** |
| 4 | negative | negative | negative |
| 5 | negative | negative | negative |
| 6 | negative | negative | negative |
| 7 | negative | negative | **subtle** |
| 8 | subtle | subtle | **clear** |
| 9 | subtle | subtle | **clear** |
| 10 | negative | subtle | **clear** |
| 11 | negative | negative | negative |
| 12 | very subtle | subtle | **clear** |
| 13 | negative | negative | **subtle** |
| 17 | **clear** | **clear** | **clear** |
| 18 | negative | negative | negative* |
| 19 | negative | negative | negative |
| 20 | negative | negative | negative |
| 22 | **clear** | subtle | **clear** |
| 25 | **very clear** | subtle | clear |
| 26 | negative | negative | **subtle** |
| 27 | post op (NA) | clear | very clear |
| 28 | clear | clear | **very clear** |
| 29 | **subtle** | negative | **subtle** |
| 30 | **very clear** | not visible | clear |
| 31 | **subtle** | not visible | not visible |
| 32 | **clear** | **clear** | **clear** |
| 33 | **subtle** | **subtle** | **subtle** |
| 34 | **clear** | subtle | **clear** |

***Table 3:*** *Clinical assessment – lesion identification results for unblinded review*

Column 'Subject' presents the subject's stratification (red for no lesion seen and green for lesion identified) based on clinical 3T epilepsy protocol and neuroradiology expert review at the time where the MPM data were acquired; Similarly, 'FLAIR', '3T R1' and 'AI Enhanced R1' columns show whether there was a lesion identified after the radiological score of how visible this lesion was on a 4 point Likert scale (not visible, subtle, clear,

medRxiv preprint doi: https://doi.org/10.1101/2025.05.23.25326669; this version posted May 23, 2025. The copyright holder for this preprint
(which was not certified by peer review) is the author/funder, who has granted medRxiv a license to display the preprint in perpetuity.
It is made available under a CC-BY-NC-ND 4.0 International license .

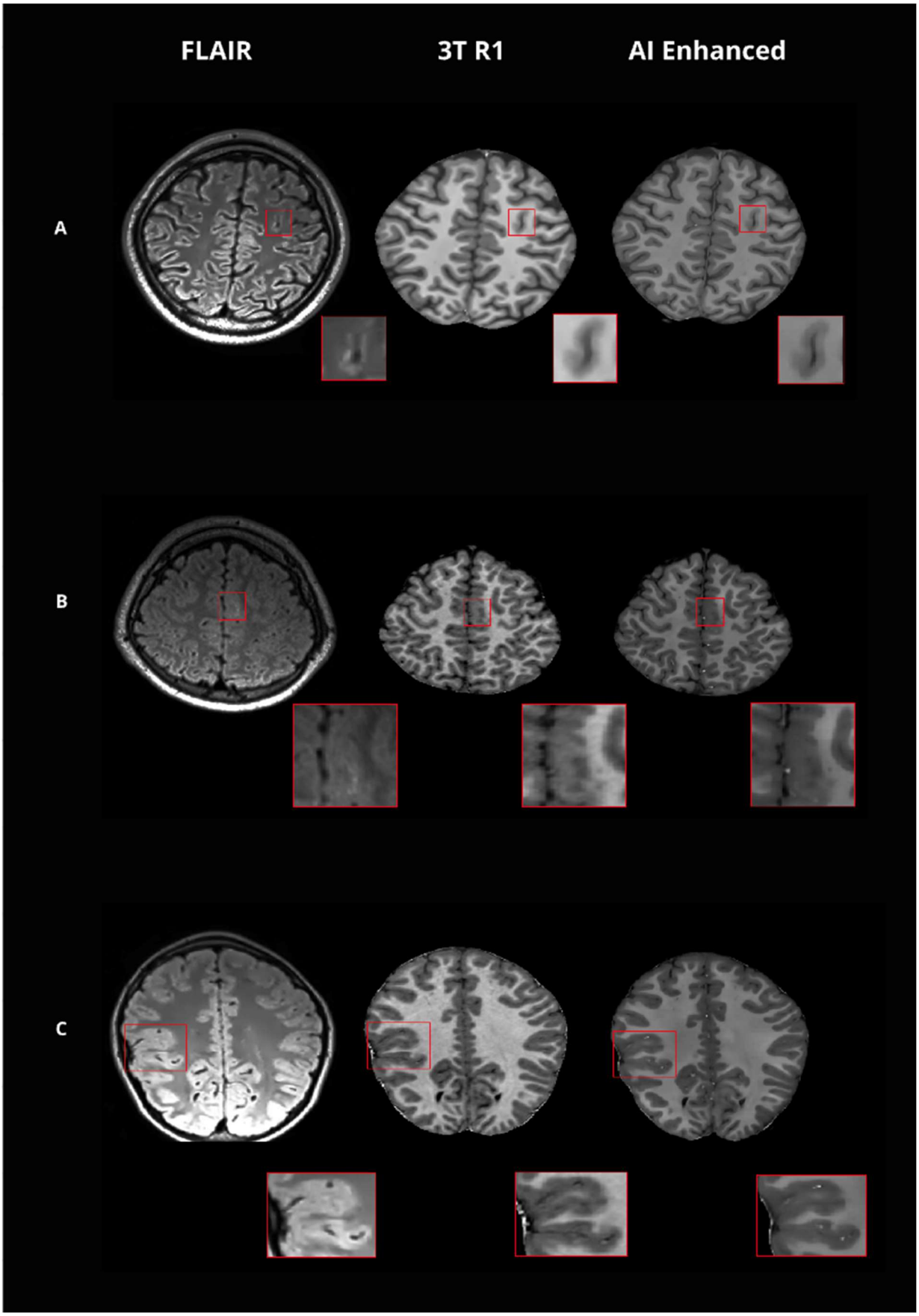



**Fig. 4:** Examples of MR positive cases (**A** (**subject 8), B** (**subject 28**)), where the visualization of the lesion with the 3T Enhanced was superior to the 3T R1 and FLAIR. Example of MR positive case (**C** (**subject 10**)), where the lesion visualization was characterized as: FLAIR 'negative', 3T 'subtle', 3T Enhanced 'clear'.

medRxiv preprint doi: https://doi.org/10.1101/2025.05.23.25326669; this version posted May 23, 2025. The copyright holder for this preprint
**(which was not certified by peer review)** is the author/funder, who has granted medRxiv a license to display the preprint in perpetuity.
It is made available under a CC-BY-NC-ND 4.0 International license .

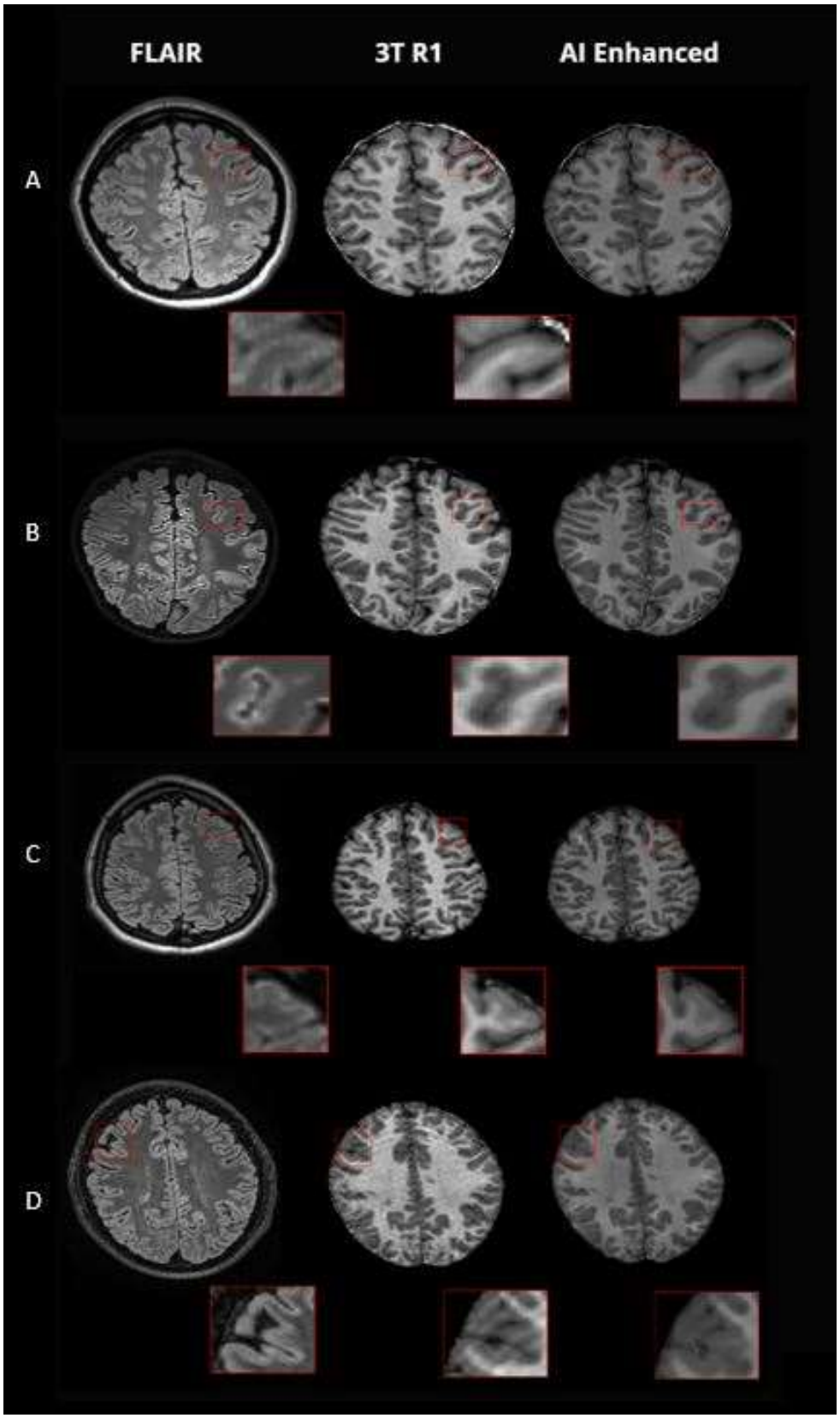



**Fig. 5. A-C** MR negative cases with lesions identified only on the AI Enhanced R1 map (**A** (**subject 7), B** (**subject 13**), **C** (**subject 26**)). **D** (**subject 29**) the MR negative subject with a lesion identified on both the AI Enhanced R1 map and 3D FLAIR.

medRxiv preprint doi: https://doi.org/10.1101/2025.05.23.25326669; this version posted May 23, 2025. The copyright holder for this preprint
**(which was not certified by peer review)** is the author/funder, who has granted medRxiv a license to display the preprint in perpetuity.
It is made available under a CC-BY-NC-ND 4.0 International license .

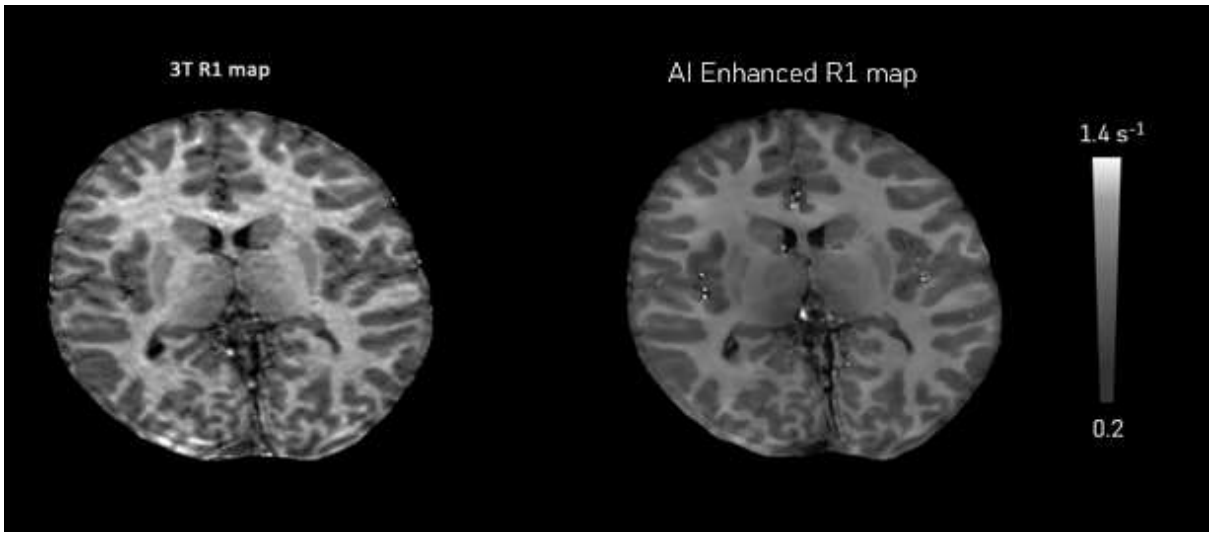



**Fig. 6:** Example of a 3T R1 map which suffers from motion artefact and the image quality has been improved on its 3T enhanced version.